The Relationship Between Ligand-Binding Thermodynamics and Protein–Ligand Interaction Forces Measured by Atomic Force Microscopy

Ashutosh Chilkoti,* Thomas Boland,‡ Buddy D. Ratner,*‡ and Patrick S. Stayton*
*Center for Bioengineering and ‡Department of Chemical Engineering, University of Washington, Seattle, Washington 98195 USA

ABSTRACT The interaction forces between biotin and a set of streptavidin site-directed mutants with altered biotin-binding equilibrium and activation thermodynamics have been measured by atomic force microscopy. The AFM technique readily discriminates differences in interaction force between the site-directed (Trp to Phe or Ala) mutants. The interaction force is poorly correlated with both the equilibrium free energy of biotin binding and the activation free energy barrier to dissociation of the biotin-streptavidin complex. The interaction force is generally well correlated with the equilibrium biotin-binding enthalpy as well as the enthalpic activation barrier, but in the one mutant where these two parameters are altered in opposite directions, the interaction force is clearly correlated with the activation enthalpy of dissociation. These results suggest that the AFM force measurements directly probe the enthalpic activation barrier to ligand dissociation.

INTRODUCTION

Molecular recognition processes, achieved by multiple noncovalent bonds between complementary binding partners, are ubiquitous in biology, encompassing interactions between proteins, protein-small molecules, and protein-DNA, and between complementary strands of DNA. The recent development of analytical techniques that can directly measure forces on a molecular scale (typically in the piconewton range) provide novel approaches to the biophysical characterization of these interactions, particularly at surfaces. These techniques include the surface force apparatus (Chen et al., 1991; Leckband et al., 1992, 1994), optical tweezers (Kuo and Sheetz, 1993; Svoboda et al., 1993), magnetic force measurement (Wang et al., 1993), pipette suction (Evans et al., 1991, 1995), and the atomic force microscope (AFM) (Binnig et al., 1986; Frommer, 1992; Quate, 1994; Rugar and Hansma, 1990). The high force sensitivity ($\sim 10^{-12}$ N), displacement sensitivity (10^{-2} nm), and the capability of operating under physiological conditions suggest that the AFM is well suited to the investigation of biological molecular recognition processes. Furthermore, the ability to map the spatial distribution of intermolecular interactions is unique to the AFM. The ability of the AFM to measure intermolecular forces has been exploited recently by several groups to investigate various phenomena at a molecular level; these include friction (Mate, 1992; Overney et al., 1992, 1994), adhesion (Burnham and Colton, 1989; Ducker et al., 1992; Hoh et al., 1992; Meyer et al., 1989; Weisenhorn et al., 1989), chemical recognition and mapping (Frisbie et al., 1994; Hoh et al., 1992), and biological molecular recognition (Boland and Ratner, 1994, in press; Dammer et al., 1995; Florin et al., 1994; Lee et al., 1994a,b; Moy et al., 1994; Pierce et al., 1994). The protein-ligand recognition studies have focused on the interaction of biotin with avidin/streptavidin as the model ligand-protein system (Florin et al., 1994; Lee et al., 1994b; Moy et al., 1994; Pierce et al., 1994) because of the high affinity and specificity of the interaction (Green, 1975), and the ease with which tips and substrates can be functionalized with complementary binding partners. The reactive, carboxy terminus of biotin allows facile immobilization of the ligand, and the 222-point symmetry of the streptavidin homotetramer allows orientation-specific immobilization of streptavidin via the biotin-binding sites present on one side of the protein, leaving free biotin-binding sites on the opposite face.

Further development of AFM as a technique for the interrogation of biological molecular recognition requires an interpretation of the measured forces in terms of the underlying biophysics of the process. We report here measurements by AFM of the biotin interaction forces for site-directed mutants of recombinant core streptavidin displaying a range of biotin-binding thermodynamic properties, and correlation of the measured forces with equilibrium and activation thermodynamic parameters of ligand binding for the various mutants. The primary advantage of this approach lies in the systematic variation of ligand-binding thermodynamics within a single protein-ligand system. Subsequent interpretation of the AFM-measured interaction forces can then be rationally approached within the context of the solution energetics of ligand binding and dissociation.

The site-directed mutagenesis studies of streptavidin have been guided by extensive structural studies on the protein. The x-ray crystal structure of apostreptavidin and biotin-bound wild-type (WT) streptavidin provides detailed structural information underlying this interaction, which includes extensive hydrogen bonding, prominent aromatic contacts, and conformational changes associated with flexible loop

Received for publication 25 May 1995 and in final form 24 July 1995.
Address reprint requests to Dr. Patrick S. Stayton, Center for Bioengineering, University of Washington, Seattle, WA 98195. Tel.: 206-685-8148; Fax: 206-685-8256; E-mail: stayton@bioeng.washington.edu.

0006-3495/95/11/2125/00 $2.00

closure and quaternary structural alterations (Hendrickson et al., 1989; Weber et al., 1989, 1992). Additionally, computational studies have suggested that the four Trp residues in contact with biotin contribute significantly to the large equilibrium free energy of biotin association (Miyamoto and Kollman, 1993a,b). We have therefore used site-directed mutagenesis to alter Trp79, Trp108, and Trp120 to Phe or Ala residues at the biotin-binding site (Chilkoti et al., 1995). These proteins display a range of equilibrium and activation thermodynamic properties, including an interesting case where the equilibrium and activation thermodynamic properties are altered in opposite directions (Chilkoti et al., 1995; Chilkoti and Stayton, in press), allowing their contributions to the AFM interaction force to be elucidated.

MATERIALS AND METHODS

Protein expression

The design and mutagenesis of the recombinant core streptavidin gene, its overexpression in *Escherichia coli* in a T7 expression system (pET-21a, Novagen, Madison, WI), and the isolation, refolding, purification, structural and biophysical functional characterization of WT streptavidin, and the Trp to Phe site-directed mutants have been reported previously (Chilkoti et al., 1995; Chilkoti and Stayton, in press). The site-directed mutants are identified as WxF or WxA, indicating a Trp to Phe or Trp to Ala mutation at residue x in the primary amino acid sequence of streptavidin. The residues are specified by their single-letter amino acid code: Trp (W), Phe (F), and Ala (A).

Streptavidin-biotin equilibrium and activation thermodynamic measurements

A detailed description of the biotin-binding equilibrium thermodynamics and biotin dissociation kinetics will appear elsewhere (Chilkoti and Stayton, in press). Briefly, the biotin-binding equilibrium free energy for the streptavidin mutants with respect to WT streptavidin ($\Delta\Delta G°$) was estimated from an enzyme-linked immunosorbent assay, and the biotin-binding equilibrium enthalpies ($\Delta H°$) for WT streptavidin and the streptavidin mutants were determined by isothermal titration calorimetry. The activation thermodynamic parameters ($\Delta H^{\neq}$ and $\Delta S^{\neq}$) for the dissociation of the biotin-streptavidin complex were determined by applying transition state theory to the experimentally measured temperature-dependent biotin dissociation kinetics.

Preparation of samples

Si_3N_4 AFM tips (Digital Instruments, Santa Barbara, CA) were sputter-coated with Au. Freshly cleaved muscovite mica and the Au-modified AFM tips were incubated overnight in a 0.15 mg ml^{-1} solution of biotin-functionalized bovine serum albumin (biotin-BSA) (Sigma Chemicals, St. Louis, MO) in phosphate-buffered saline (PBS), pH 7.0, at 4°C. The tip and the substrate were washed repeatedly in buffer and stored in PBS until use. The biotin-BSA-functionalized mica substrate was then incubated in a 0.02 mg ml^{-1} solution of WT streptavidin or Trp site-directed mutants for at least 1 h at room temperature. Samples were then rinsed with PBS and assayed immediately with AFM. These conditions result in saturation coverage for all streptavidin variants (Chilkoti et al., 1995). There are several advantages of using biotin-BSA adsorbed on mica: first, BSA is known to irreversibly adsorb on mica, such that the magnitude of the AFM forces do not result in detachment of the biotin-BSA molecules from the tip; and second, biotin groups allow orientation-specific attachment of streptavidin to the substrate.

Atomic force microscopy

The AFM experiments were carried out on a Nanoscope II instrument (Digital Instruments) in the force scan mode. The cantilever deflection upon approach to the substrate and retraction was measured and recorded, and averaged on a digital storage oscilloscope. The oscilloscope averages the last 100 scans before storage. The force of detachment was extracted from the force scan by means of the independently ascertained force constant of the cantilever, determined by the end mass resonance method (Hutter and Bechhoefer, 1993). The force constants for experiments (a) and (b) in Table 2 were 0.064 N m^{-1} and 0.039 N m^{-1}, respectively. Three or more averaged force curves (100 scans each) were independently captured with the digital storage oscilloscope for each streptavidin variant, and the force of detachment for each averaged force curve was determined and then averaged to yield the force and associated standard deviation for each streptavidin variant. This experimental procedure was followed for each streptavidin variant in the absence of, and then in the presence of, free biotin in the imaging buffer to determine the total force, and nonspecific force, respectively. The specific force is the difference between the total force and nonspecific force measured for each streptavidin variant, and the reported uncertainty is calculated from the standard deviation associated with the experimentally measured total force and nonspecific force.

RESULTS AND DISCUSSION

AFM tips were first deposited with Au and then functionalized with biotin by adsorption of biotin-BSA. The substrate, freshly cleaved muscovite mica, was similarly incubated in biotin-BSA, followed by WT streptavidin or a mutant. Ligand-protein interaction forces were measured with the AFM in the force scan mode. Substrates functionalized with different mutants were sequentially assayed in the absence of and then in the presence of biotin to provide the specific biotin interaction force for each mutant. The same tip was used across the entire protein series to minimize potential errors that can arise from several sources. First, using the same AFM tip for the entire series of streptavidin variants eliminates the variation observed in the absolute force measured using different tips, which we believe arises largely from variations in tip geometry (e.g., see entries (a) and (b) in Table 1 for WT streptavidin using two different tips). Although variations in the surface density of biotin on the AFM tip can contribute to the observed variability in the absolute measured force using different tips, this effect can be minimized by functionalizing tips with biotin under experimentally invariant conditions. We also note that the variation in surface density of ligand is not an issue if the same tip is used for all proteins. An additional source of error, arising from variations in streptavidin surface density, has been minimized by preparing all samples in the same manner while ensuring saturation coverage of protein on the substrate.

An averaged force scan for the interaction of a biotin-functionalized tip with WT streptavidin is shown in Fig. 1 (lower force curve). The force scan measured upon blocking the biotin-binding sites for the same sample-tip combination by preincubating the streptavidin substrate in free biotin is also shown in Fig. 1 (upper force curve) and is observed to be significantly lower. The specific force of interaction (ΔF) for WT streptavidin and the Trp mutants, reported in

TABLE 1 Summary of the force of detachment (in pN) measured between biotin-functionalized tips and streptavidin (WT or mutant)-functionalized samples

Protein	Specific force (pN) [ΔF]	ΔΔF (pN)
WT streptavidin	(a) 253 ± 20	0
	(b) 393 ± 10	
W79A	(a) 158 ± 17	−95
	(b) 332 ± 31	−61
W79F	(a) 294 ± 10	+41
	(b) 439 ± 11	+46
W108F	(b) 443 ± 33	+50
W120A	(b) 257 ± 28	−300
W120F	(b) 92 ± 19	−136

The specific force of detachment is the difference between the total measured force of interaction and the residual force measured upon blocking of biotin-binding sites by free biotin present in excess in the imaging buffer. The data were obtained by averaging the results from 100 force-versus-displacement curves for each sample.
(a) and (b) refer to two independent experiments performed with different tips. $\Delta\Delta F = \Delta F(\text{mutant}) - \Delta F(\text{WT})$.

Table 1, is the difference between the total force measured in the absence of biotin and the residual force measured in the presence of free biotin in the imaging buffer. The specific force of biotin detachment for the various mutants varied from 90 to 400 pN, and the average nonspecific force for all experiments was 105 ± 60 pN. The force of detachment for WT streptavidin ascertained in two independent experiments with different tips varied significantly, most likely because of differences in tip geometry. To minimize this variation across different experiments, we have used the difference force parameter $\Delta\Delta F$ [$\Delta\Delta F = \Delta F(\text{mutant}) - \Delta F(\text{WT})$], which normalizes the specific forces for the different mutants with respect to WT streptavidin for each independent set of experiments. Additionally, this facilitates comparison of the AFM results for the different mutants with the corresponding thermodynamic alterations, all of which were determined relative to WT streptavidin.

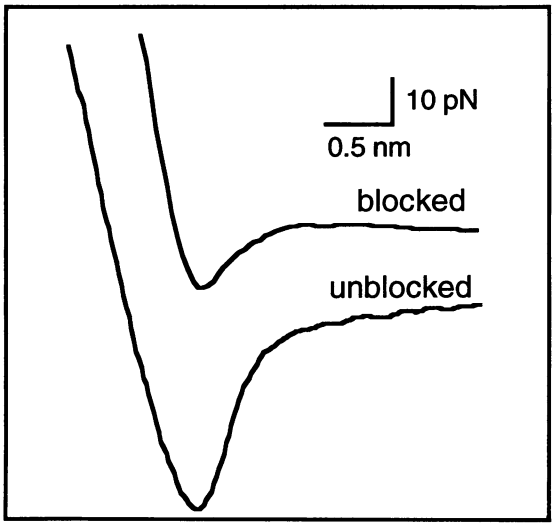

FIGURE 1 Typical force versus displacement curves recorded between a biotin-functionalized tip and WT streptavidin sample in PBS, pH 7.0, at room temperature, with a Nanoscope II atomic force microscope. The force curve shown here is the averaged force curve from 100 individual scans. The bottom curve is the force curve with the biotin-binding sites in the protein accessible to the biotin-functionalized tip, and the top curve is the force curve with the biotin-binding sites in the protein pre-blocked with free biotin in the buffer.

The biotin-binding equilibrium thermodynamic parameters [free energy ($\Delta G°$), enthalpy ($\Delta H°$)] and the activation thermodynamic barriers for dissociation of the biotin-streptavidin complex ($\Delta G^{\neq}$ and $\Delta H^{\neq}$) for WT streptavidin are shown in Table 2. A detailed discussion of these measurements will appear elsewhere (Chilkoti and Stayton, in press). Thermodynamic difference parameters for the site-directed Trp mutants ($\Delta\Delta X = \Delta X(\text{mutant}) - \Delta X(\text{WT})$, where ΔX is the equilibrium or activation thermodynamic parameter of interest) are also reported in Table 2. No correlation is observed between either $\Delta\Delta G°$ or $\Delta\Delta G^{\neq}$ and $\Delta\Delta F$ for the different streptavidin mutants ($R^2 < 0.8$). However, both the biotin-binding equilibrium difference enthalpy ($\Delta\Delta H°$) and the difference activation enthalpic barrier to biotin dissociation ($\Delta\Delta H^{\neq}$) correlate with $\Delta\Delta F$ (Fig. 2, *a* and *b*, respectively). There is an important exception to this trend: the activation enthalpy for dissociation ($\Delta H^{\neq}$) and the equilibrium biotin-binding enthalpy ($\Delta H°$) for W108F are altered in opposite directions, relative to WT streptavidin. The larger interaction force for W108F, relative to WT streptavidin ($\Delta\Delta F = +50$ pN), correlates with the increased activation enthalpic barrier ($\Delta\Delta H^{\neq} = +4.5$ kcal mol^{-1}) but not with the decreased equilibrium biotin-binding enthalpy ($\Delta\Delta H° = +1.0$ kcal mol^{-1}).

The force of interaction measured in the AFM experiment is the force of detachment of the biotin-functionalized AFM tip from the streptavidin-functionalized substrate. The correlation of this force of interaction with the enthalpic parameters and not with the free energy parameters suggests that the AFM is insensitive to the entropic changes associ-

TABLE 2 Summary of biotin-binding equilibrium thermodynamic difference parameters and activation thermodynamic difference parameters of streptavidin-biotin dissociation for WT streptavidin and Trp site-directed mutants at 298 K

Protein	$\Delta\Delta G°$	$\Delta\Delta H°$	$\Delta\Delta G^{\neq}$	$\Delta\Delta H^{\neq}$
WT streptavidin	$\Delta G° = -18.3$	$\Delta H° = -24.5$ ±0.5	$\Delta G^{\neq}$ 24.4 ± 2.4	$\Delta H^{\neq} = 32$ ± 2.1
	$\Delta\Delta G° = 0$	$\Delta\Delta H° = 0$	$\Delta\Delta G^{\neq} = 0$	$\Delta\Delta H^{\neq} = 0$
W79A	+7.6	+6.0	ND	ND
W79F	0.8	−1.5	−1.1	+2.9
W108F	0.5	+1.0	−1.7	+4.5
W120A	+8.8	+11.7	ND	ND
W120F	2.7	+5.1	−2.5	−3.5

$\Delta\Delta X = \Delta X(\text{mutant}) - \Delta X(\text{WT})$, where ΔX is a thermodynamic parameter of interest. ND, not determined. The biotin-dissociation kinetics of these mutants are too rapid to allow determination of the activation thermodynamic parameters by the methods utilized for the other mutants in this study. All thermodynamic parameters are in kcal mol^{-1}.

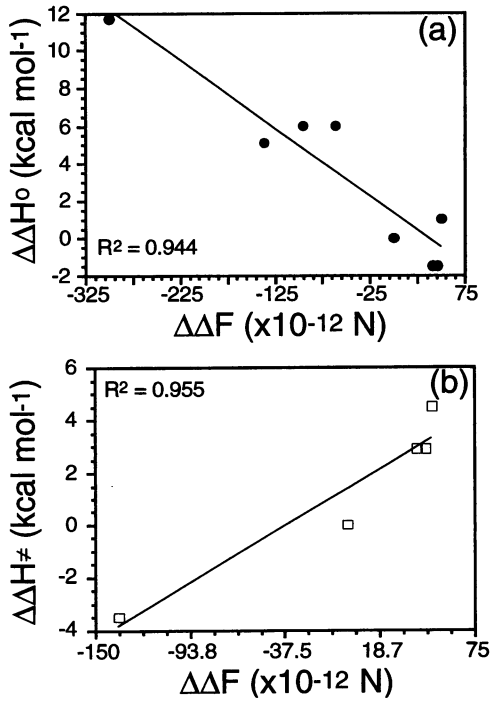

FIGURE 2 Plot of specific differential force of interaction between the Trp mutants and biotin measured by AFM and biotin-binding thermodynamic parameters. (*a*) Difference equilibrium enthalpy ($\Delta\Delta H°$); (*b*) difference activation enthalpy of dissociation ($\Delta\Delta H^{\neq}$).

ated with ligand dissociation, as suggested previously (Florin et al., 1994; Moy et al., 1994). Their studies indicated that the intermolecular forces between streptavidin/avidin, and biotin and its congeners correlate with the thermodynamics of ligand binding, specifically the equilibrium biotin-binding enthalpy. However, the AFM-measured protein-ligand forces were only compared with equilibrium thermodynamic parameters. The linear correlation observed in that study between the AFM-measured force and equilibrium biotin-binding enthalpy also depends on the use of a streptavidin-biotin enthalpy of -32 kcal mol^{-1} (Weber et al., 1992), which has been more recently measured at -24.5 kcal mol^{-1} (Chilkoti and Stayton, in press).

It is important to note that the correlation of $\Delta\Delta F$ with alterations in biotin-binding equilibrium enthalpy ($\Delta\Delta H°$) does not necessarily imply that the force curves reflect a sampling of the equilibrium enthalpic potential surface. Clarifying the relationship between the AFM-measured interaction force and the enthalpic parameters requires consideration of the correlation that may exist between alterations in the biotin-binding activation enthalpy and equilibrium enthalpy. There are two limiting cases for the thermodynamic alterations ensuing from a binding-site mutation: one in which the effect of the mutation, relative to WT protein, results solely in thermodynamic alterations in the ligand-bound state, and another in which the mutation affects only the transition state for ligand dissociation, leaving the ligand-bound state unperturbed. The thermodynamic profiles for ligand binding and dissociation corresponding to these limiting cases are shown in Fig. 3. The activation barrier difference parameter, $\Delta\Delta X^{\neq}$, arising from a site-specific mutation, can be partitioned between transition state alterations ($\Delta\Delta X^{TS}$) and ground state alterations ($\Delta\Delta X°$), relative to the WT protein, as follows:

$$\Delta\Delta X^{\neq} = \Delta\Delta X^{TS} - \Delta\Delta X° \quad (1)$$

The negative sign before $\Delta\Delta X°$ is due to the convention of referencing the equilibrium thermodynamic parameters to the free ligand and protein, whereas the activation parameters are referenced to the ligand-bound protein. For the former case (Fig. 3, profile *A*), because $\Delta\Delta X°$ and $\Delta\Delta X^{\neq}$ are perfectly correlated ($\Delta\Delta X^{TS} = 0$), in the event that a correlation exists, $\Delta\Delta F$ will correlate with both $\Delta\Delta X^{\neq}$ and $\Delta\Delta X°$. In the latter case, however, $\Delta\Delta F$ will correlate with $\Delta\Delta X^{\neq}$ and not with $\Delta\Delta X°$, because $\Delta\Delta X°$ is zero and the thermodynamic effect of the mutation is manifested solely in the transition state ($\Delta\Delta X^{\neq} = \Delta\Delta X^{TS}$; Fig. 3, profile *B*).

The thermodynamic profiles of site-directed mutations can lie at either end of this spectrum, or lie somewhere between these two limiting cases, i.e., partitioned between

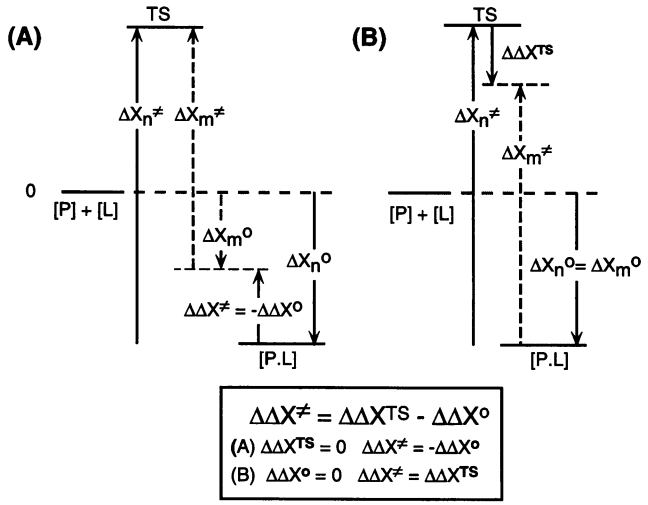

FIGURE 3 Schematic of ligand-binding thermodynamic diagram of native protein and a ligand-binding site-directed mutant. Two limiting cases are shown: (*A*) The site-directed mutation alters the ligand-bound protein state, with no effect on the transition state. The altered thermodynamics of the system are reflected solely in the the equilibrium thermodynamic parameters ($\Delta X_n° \neq \Delta X_m°$; $\Delta\Delta X° \neq 0$); and not in transition state parameters (i.e., $\Delta X_n^{\neq} = \Delta X_m^{\neq}$; $\Delta\Delta X^{\neq} = 0$). (*B*) The site-directed mutation alters the transition state, with no effect on the ligand-bound protein. The altered thermodynamics of the system are reflected solely in the transition state parameters (i.e., $\Delta X_n^{\neq} \neq \Delta X_m^{\neq}$; $\Delta\Delta X^{\neq} \neq 0$) and not in the equilibrium thermodynamic parameters ($\Delta X_n° = \Delta X_m°$; $\Delta\Delta X° = 0$). The broken vertical arrows indicate the relevant thermodynamic parameter of interest (equilibrium or activation) for the mutant, and the unbroken vertical arrows indicate the corresponding thermodynamic parameter for WT (native) protein. The energy diagram is referenced to the unbound protein [P] and free ligand [L] as zero. ΔX is the thermodynamic parameter of interest, $\Delta\Delta X$ is the equivalent difference parameter defined as ΔX(mutant) $-$ ΔX(native), subscripts n and m refer to native and mutant protein respectively, superscipts ° and $^{\neq}$ refer to ligand-bound equilibrium [P.L.] and transition state [TS], respectively.

ground state and transition state alterations. It is apparent from Table 2 that W120F is largely altered in the ligand-bound state and is closer to case (A) than case (B) in Fig. 3. The 3.5 kcal mol^{-1} decrease in the enthalpic barrier to dissociation, relative to WT streptavidin ($\Delta\Delta H^{\neq} = -3.5$ kcal mol^{-1}), is largely accounted for by the 5.1 kcal mol^{-1} destabilization of the ligand-bound W120F ($\Delta\Delta H° = +5.1$ kcal mol^{-1}). The enthalpic alterations with the W79F mutation arise from changes in both the ligand-bound state and the transition state, and the profile of this mutant is thus intermediate between (A) and (B) in Fig. 3. The enthalpic barrier to dissociation, relative to WT streptavidin, increases by 2.9 kcal mol^{-1} ($\Delta\Delta H^{\neq} = +2.9$ kcal mol^{-1}) and is due to a 1.5 kcal mol^{-1} stabilization of the ligand-bound state of W79F ($\Delta\Delta H° = -1.5$ kcal mol^{-1}) and a 1.4 kcal mol^{-1} destabilization of the transition state ($\Delta\Delta H^{TS} = +1.4$ kcal mol^{-1}), relative to WT streptavidin. Because $\Delta\Delta H°$ and $\Delta\Delta H^{\neq}$ are correlated both with each other and with $\Delta\Delta F$ for W79F and W120F, the relationship between the differential force of interaction and alterations in the equilibrium enthalpy and activation enthalpic barriers cannot be easily separated.

The W108F mutation, however, largely affects the energetics of the transition state. The increased activation enthalpic barrier of +4.5 kcal mol^{-1}, relative to WT streptavidin, is dominated by the +5.5 kcal mol^{-1} destabilization of the transition state ($\Delta\Delta H^{TS} = +5.5$ kcal mol^{-1}), with a small and opposing change in $\Delta\Delta H°$ (+1 kcal mol^{-1}). Thus the larger force measured for W108F, relative to WT streptavidin ($\Delta\Delta F = +50$ pN), correlates with the increased activation enthalpic barrier ($\Delta\Delta H^{\neq} = +4.5$ kcal mol^{-1}) but not with the decreased equilibrium binding enthalpy of W108F ($\Delta\Delta H° = +1$ kcal mol^{-1}) (Fig. 4). These results suggest that the AFM detachment process is sampling the enthalpic barrier to dissociation, and that the apparent correlation with $\Delta H°$ arises because changes in the enthalpy level of the ligand-bound state are often folded into the magnitude of the activation enthalpy.

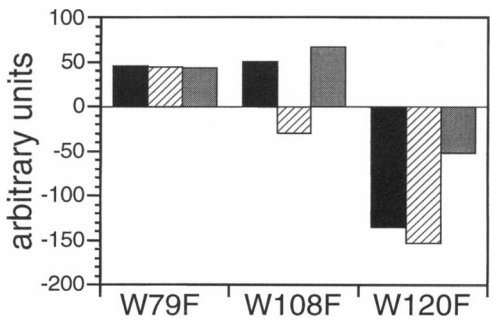

FIGURE 4 Bar graph of the specific force of interaction and the difference thermodynamic parameters for W79F, W108F, and W120F; $\Delta\Delta F$ (filled bars), $\Delta\Delta H°$ (hatched bars), $\Delta\Delta H^{\neq}$ (shaded bars). $\Delta\Delta H°$ is plotted as $-15x\Delta\Delta H°$ and $\Delta\Delta H^{\neq}$ is plotted as $30x\Delta\Delta H^{\neq}$ to report the results on the same scale as $\Delta\Delta F$.

CONCLUSIONS

We have demonstrated here that the AFM can be used to characterize the differential biotin interaction forces arising from site-specific, single-residue alterations in the biotin-binding site of streptavidin. The correlation of the AFM-measured interaction forces with enthalpic difference parameters and not with free energy suggests that the force measurements directly probe the internal energy associated with the bond-breaking activation processes and not the entropy change associated with ligand dissociation (which arises from changes in the translational and rotational degrees of freedom of ligand and protein, dilution effects, changes in protein conformation, and solvent reorganization) (Spolar and Record, 1994; Vajda et al., 1994). Although these initial experiments have provided a key link between the AFM rupture force and solution thermodynamics, many questions regarding the energetics and detailed reaction trajectories remain to be elucidated. More sophisticated computational simulation of the unbinding energetics and further experimentation with new mutants separating the equilibrium and activation thermodynamics should clarify many of these questions. Finally, expanding these studies to include complementary experimental sytems where ligand binding is dominated by entropic processes rather than enthalpy should further clarify the relationship between solution thermodynamic parameters and the AFM-measured forces.

This work was supported by National Institutes of Health grant RR01296 (BDR) and by the National Science Foundation (PSS) and the Whitaker Foundation (PSS). We acknowledge the Biocalorimetry Center, Department of Biology, Johns Hopkins University, for the biotin-binding equilibrium enthalpy measurements of the streptavidin variants.

REFERENCES

Binnig, G., C. F. Quate, and C. Gerber. Atomic force microscope. 1986. *Phys. Rev. Lett.* 56:930–933.

Boland, T., and B. D. Ratner. 1994. Two dimensional assembly of purines and pyrimidines on Au(111). *Langmuir.* 10:3845–3852.

Boland, T., and B. D. Ratner. 1995. Direct measurement by atomic force microscopy of hydrogen bonding in DNA nucleotide bases. *Proc. Natl. Acad. Sci. USA.* 92:5297–5301.

Burnham, N. A., and R. J. Colton. Measuring the nanomechanical properties, and surface forces of materials using an atomic force microscope. 1989. *J. Vac. Sci. Tech. A.* 7:2906–2913.

Chen, Y.-L., C. A. Helm, and J. N. Israelachvili. 1991. Molecular mechanisms associated with adhesion and contact angle hysteresis of monolayer surfaces. *J. Phys. Chem.* 95:10736–10747.

Chilkoti, A., and P. S. Stayton. Molecular origins of the slow streptavidin-biotin dissociation kinetics. *J. Am. Chem. Soc.* In press.

Chilkoti, A., P. H. Tan., and P. S. Stayton. 1995. Site-directed mutagenesis studies of the high-affinity streptavidin-biotin complex: contributions of tryptophan residues 79, 108, and 120. *Proc. Natl. Acad. Sci. USA.* 92:1754–1758.

Dammer, U., O. Popescu, P. Wagner, D. Anselmetti, H.-J. Güntherodt, and G. N. Misevic. 1995. Binding strength between cell adhesion proteoglycans measured by atomic force microscopy. *Science.* 267:1173–1175.

Ducker, W. A., T. J. Senden, and R. M. Pashley. 1992. Measurement of forces in liquids using a force microscope. *Langmuir.* 8:1831–1836.

Evans, E., D. Berk, and A. Leung. 1991. Detachment of agglutinin-bonded red blood cells. I. Forces to rupture molecular point attachments. *Biophys. J.* 59:838–848.

Evans, E., K. Ritchie, and R. Merkel. 1995. Sensitive force technique to probe molecular adhesion and structutal linkages at biological interfaces. *Biophys. J.* In press.

Florin, E.-L., V. T. Moy, and H. E. Gaub. 1994. Adhesion forces between individual ligand-receptor pairs. *Science.* 264:415–417.

Frisbie, C. D., L. F. Rozsnyai, A. Noy, M. S. Wrighton, and C. M. Lieber. 1994. Functional group imaging by chemical force microscopy. *Science.* 265:2071–2074.

Frommer, J. 1992. Scanning tunneling microscopy and atomic force microscopy in organic chemistry. *Angew. Chem. Int. Ed. Engl.* 31: 1298–1328.

Green, N. M. 1975. Avidin. *Adv. Protein Chem.* 29:85–133.

Hendrickson, W. A., A. Pahler, J. L. Smith, Y. Satow, E. A. Meritt, and R. P. Phizackerley. 1989. Crystal structure of core streptavidin determined from multiwavelength anomalous diffraction of synchrotron radiation. *Proc. Natl. Acad. Sci. USA.* 86:2190–2194.

Hoh, J. H., J. P. Cleveland, C. B. Prater, J. P. Revel, and P. K. Hansma. 1992. Quantized adhesion detected with the atomic force microscope. *J. Am. Chem. Soc.* 114:4917–4918.

Hutter, J. L., and J. Bechhoefer. 1993. Calibration of atomic-force microscope tips. *Rev. Sci. Instrum.* 64:1868–1873.

Kuo, S. C., and M. P. Sheetz. 1993. Force of single kinesin molecules measured with optical tweezers. *Science.* 260:232–234.

Leckband, D. E., J. N. Israelachvili, F.-J. Schmitt, and W. Knoll. 1992. Long range attraction and molecular rearrangements in receptor-ligand interactions. *Science.* 255:1419–1421.

Leckband, D. E., F.-J. Schmitt, J. N. Israelachvili, and W. Knoll. 1994. Direct force measurements of specific and nonspecific protein interactions. *Biochemistry.* 33:4611–4623.

Lee, G. U., L. A. Chrisey, and R. J. Colton. 1994a. Direct measurement of the forces between complementary strands of DNA. *Science.* 266: 771–773.

Lee, G. U., D. A. Kidwell, and R. J. Colton. 1994b. Sensing discrete streptavidin-biotin interactions with atomic force microscopy. *Langmuir.* 10:354–357.

Mate, C. M. 1992. Study of polymer lubrication on sillicon surfaces. *Phys. Rev. Lett.* 68:3323–3326.

Meyer, E., H. Heinzelmann, P. Grutter, T. Jung, H.-R. Hidber, H. Rudin, and H.-J. Güntherodt. 1989. Atomic force microscopy for the study of tribology and adhesion. *Thin Solid Films.* 181:527–544.

Miyamoto, S., and P. Kollman. 1993a. Absolute and relative binding free energy calculations of the interction of biotin and its analogs with streptavidin using molecular dynamics/free energy perturbation approaches. *Proteins.* 16:226–245.

Miyamoto, S., and P. Kollman. 1993b. What determines the strength of noncovalent association of ligands to proteins in aqueous solution? *Proc. Natl. Acad. Sci. USA.* 90:8402–8406.

Moy, V. T., E.-L. Florin, and H. E. Gaub. 1994. Intermolecular forces and energies between ligands and receptors. *Science.* 266:257–259.

Overney, R. M., E. Meyer, J. Frommer, D. Brodbeck, R. Lüthi, L. Howald, M.-J. Güntherodt, M. Fujihara, H. Takano, and Y. Gotoh. 1992. Friction measurements on phase-separated thin fims with a modified atomic force microscope. *Nature.* 359:133–135.

Overney, R. M., E. Meyer, J. Frommer, M.-J. Güntherodt, M. Fujihara, H. Takano, and Y. Gotoh. 1994. Force microscopy of friction and elastic compliance of phase-separated organic thin films. *Langmuir.* 10: 1281–1286.

Pierce, M., J. Stuart, A. Pungor, P. Dryden, and V. Hlady. 1994. Adhesion force measurements using an atomic force microscope with a linear position sensitive detector. *Langmuir.* 10:3217–3221.

Quate, C. F. 1994. The AFM as a tool for surface imaging. *Surf. Sci.* 299/300:980–995.

Rugar, D., and P. Hansma. 1990. Atomic force microscopy. *Phys. Today* 43:23–30.

Spolar, R. S., and M. T. Record, Jr. 1994. Coupling of local folding to site-specific binding of proteins to DNA. *Science.* 263:777–784.

Svoboda, K., C. F. Schmidt, B. J. Schnapp, and S. M. Block. 1993. Direct observation of kinesin stepping by optical trapping interferometry. *Nature.* 365:721–727.

Vajda, S., Z. Weng, R. Rosenfeld, and C. DeLisi. 1994. Effect of conformational flexibility and solvation on receptor-ligand binding free energies. *Biochemistry.* 33:13977–13988.

Wang, N., J. P. Butler, and D. E. Ingber. 1993. Mechanotransduction across the cell surface and through the cytoskeleton. *Science.* 260: 1124–1127.

Weber, P. C., D. H. Ohlendorf, J. J. Wendoloski, and F. R. Salemme. 1989. Structural origins of high-affinity biotin binding to streptavidin. *Science.* 243:85–88.

Weber, P. C., J. J. Wendoloski, M. W. Pantoliano, and F. R. Salemme. 1992. Crystallographic and thermodynamic comparison of natural and synthetic ligands bound to streptavidin. *J. Am. Chem. Soc.* 114: 3197–3200.

Weisenhorn, A. L., P. K. Hansma, T. R. Albrecht, and C. F. Quate. 1989. Forces in atomic force microscopy in air and water. *Appl. Phys. Lett.* 54:2651–2653.